Automated Defect Detection: Computational Methods to Detect Flaws in Industrial Parts

Charlie Brummitt (University of California at Davis)
Claudette Foisy (Clarkson University)
Garry Halliwell (State University of New York at Buffalo)
Michael Higley (New Jersey Institute of Technology)
Seyfullah Kotil (Rensselaer Polytechnic Institute)
Peter R. Kramer (Rensselaer Polytechnic Institute)
Martial Longla (University of Cincinnati)
Matthew Reyna (Rensselaer Polytechnic Institute)

Project Sponsors: J. Brandon Laflen and Bob Kaucic
Visualization and Computer Vision Laboratory, GE

July 16, 2011

1 Introduction and Motivation

The problem brought to the MPI workshop by representatives from the GE Visualization and Computer Vision Laboratory concerned the rapid automatic identification of defects in industrial parts based on digitized images captured from X-ray scans [12]. Key defect types of concern include:

- void regions, which could be caused by liquid metal flowing too slowly during the casting process to equilibrate its density (Figure 1),

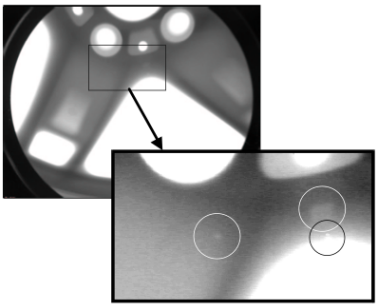

Figure 1: 3 voids in aluminum (aluminium) wheel [12])

- fractures, which could be caused by mechanical stresses in response to temperature gradients, and
- undesired inclusions, such as sand failing to evacuate a region which should be free of material.

GE has defect detection algorithms based on nonparametric statistical fitting, trained on data sets, which work well for two-dimensional data, but their extension to three-dimensional scans is unclear. The goal of the working group was to try to formulate some novel approaches to detecting defects in three-dimensional scans of the parts. Quantitatively, we are presented with an image represented as a three-dimensional array of voxels (volumetric picture elements), each of which has an intensity value associated to it. This intensity refers to the amount of radiation scattered from that voxel to the imaging apparatus, as estimated by an algorithm which reconstructs the three-dimensional image from the radiation measurements received by the camera. While the reconstruction algorithm used by GE is state-of-the art, we must keep in mind that it does introduce some noise and inaccuracies. The goal of an automated detection algorithm is to identify the location of defects (if any) in the test part, given the three-dimensional array of intensity data for a test part, together perhaps with whatever information we desire from an ideal reference for the part. The quantitative operational goals are that 95% of all defects are found, no more than one false positive defect is identified per part, and that the algorithm does not require more than on the order of one minute per part inspected.

In this report, we summarize the ideas and developments which emerged from the interaction of the GE representatives with the academic partici-

pants at the workshop. We begin in Section 2 with some statistical analysis of the noise in the images as inferred from a collection of images of different instances of a given part. The purpose of quantifying the properties of the noise is twofold: 1) to give some idea of the challenge the imaging noise presents in identifying defects, and 2) to provide a basis for a statistical model for the noise that could be used in a probabilistically-based detection algorithm. Next, in Section 3, we present a mathematical toy model for defective part images which seems to have many of the key features in the real part images. Such a simplified mathematical model can be helpful in developing image detection algorithms because all its details are available to us. In particular, in the mathematical model, we know (by construction of the model) whether an aberration detected by the algorithm is associated to a real defect or to a noisy intensity fluctuation or image reconstruction artifact. Such detailed information may not be inferrable from the actual images. Moreover, the mathematical model has many easily adjustable parameters, which can help us determine for which regimes a given detection algorithm works well. For example, we can vary at will the sizes of defects, the level of the imaging noise, and the thickness of the sample. We then present three conceptual approaches to defect detection which were discussed during the workshop. First, in Section 4, we present a geometric approach in which a reference surface is generated which separates the interior of the part (which should be metallic) from the exterior (which should be air). The interior region is tested for the presence of anomalously low intensity (corresponding to a putative undesired void), while the exterior region is tested for the presence of anomalously high intensity (corresponding to the presence of undesired material). Next, in Section 5, we sketch an idea for expanding the voxel data with respect to a suitable orthonormal basis of functions, some of which are characteristic of defects. Curvelets [2, 19] seem like a promising candidate, in that they can identify the presence of suspicious geometric features. Third, in Section 6, we briefly present an idea for detecting occlusions to void regions, by examining whether the topology of the test images is consistent with that of the ideal reference. We finally conclude in Section 7 with some suggestions for future investigation.

2 Noise Model

As one of the objectives is for the defect detection algorithm to be robust against the noise arising from the imaging process, we examined the statistics of the noise from some sample images. We expect, and do find, that the level of noise is dependent on the expected intensity of a voxel. For clarity, we work with a normalized intensity variable I ranging from 0 to 1, where the value 1 corresponds to the maximum intensity observed in a pixel. This maximum intensity may be interpreted as the ideal intensity corresponding to a voxel that is entirely filled with material. Ideally, void regions should return 0 intensity values. The imaging process and the algorithm used to approximately reconstruct the actual image from the raw image will create deviations from this ideal intensity profile in the following ways:

- Voxels containing material deep below the surface will be represented with a reduced intensity due to scattering and absorption of photons by intervening material (photon starvation)
- The reconstruction algorithm will tend to blur the intensity of a voxel with those of neighboring voxels. Therefore, voxels near edges between material and void regions can be expected to exhibit intensity values somewhat between 0 and 1.

Taking into account these imaging issues as well as the fact that the images will not always be perfectly aligned with one another, the statistics of the intensity of a voxel from an image can be expected to behave as follows:

- The mean intensity will tend to be larger in material regions than in void regions, but will generally decrease in voxels that lie behind a substantial amount of material. In fact, the observed intensity of a material region deep within the part may actually be below the observed intensity of a void region near the surface.
- The standard deviation of the intensity should be most pronounced near edges, and therefore for intermediate values of the intensity. This high variability for voxels near the edges arises because the intensity observed in the voxel will be very sensitive to how exactly the edge is aligned in the given image. That is, the spatial intensity of the gradient is large here and so small spatial shifts in the image will create large changes in intensity.

These suppositions are borne out in analysis of the data of 15 images of some reference part data made available to us, with outliers removed. First, we observe in Figure 2 that the distribution of intensities observed in voxels has a bimodal shape, with the larger intensity peak presumably corresponding to material regions and the lower intensity peak corresponding to void regions. Next, in Figure 3, we present a scatterplot of the mean and standard deviation of the intensity observed in each voxel from the same set of data. We indeed observe higher variability of intensity associated with intermediate values of the mean intensity. Indeed, we can infer from this plot the following empirical model for the standard deviation σ_I (noise) in the intensity as a function of its mean value $\bar{I}$ (which we may take as the intensity value that should be observed, taking into account systematic effects like photon starvation, but neglecting fluctuations due to spatial alighment shifts, etc.):

$$\sigma_I = \begin{cases} \frac{0.15}{0.25}\bar{I}, & 0 \leq \bar{I} \leq 0.25 \\ 0.15, & 0.25 < \bar{I} < 0.75 \\ \frac{0.15}{0.25}\left(1-\bar{I}\right), & 0.75 \leq \bar{I} \leq 1 \end{cases}$$

For completeness, we also present in Figure 4 a histogram of the variance of the intensity of a voxel from the same data set. While presenting an overall sense of the level of noise, its precise details do not seem like an appropriate basis from which to develop a model or algorithm since it pools together statistics of voxels from very different regions (material, void, edges).

3 Toy Model

To aid with the development of our defect detection algorithms, we designed a "toy model" that served a twofold purpose. Firstly, we had limited access to X-ray images and CAD models because of the inherent sensitivity of sharing information about actual manufacturing defects; a toy model provided immediate and ample imagery to which we could apply our algorithms. Secondly, we had concerns about developing our algorithms with actual X-ray images because of the inherent complexity of the manufacturing defects, image reconstruction, etc.; a toy model provided the ability to model and introduce particular defects, noise, etc. as appropriate for each stage of the algorithm's development. That is, this toy model could be used to explore the merits of a defect detection algorithm apart from the question of what noise model, etc. best fits the data. A defect detection algorithm could be tested on the toy

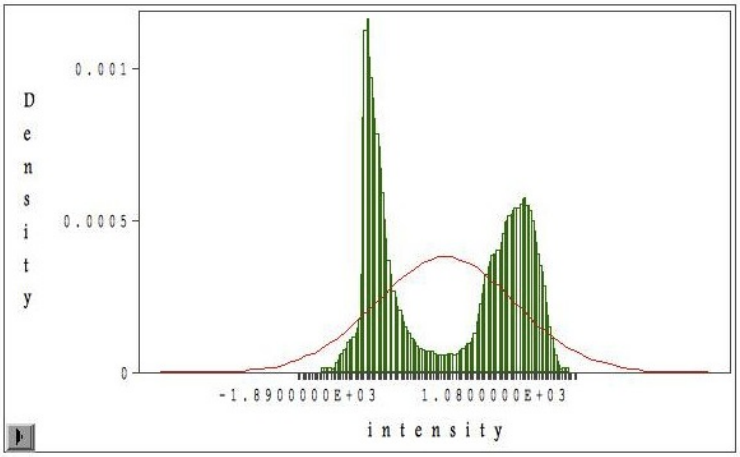

Figure 2: Histogram of intensities observed, pooled over all voxels in 15 samples of a part provided to the working group

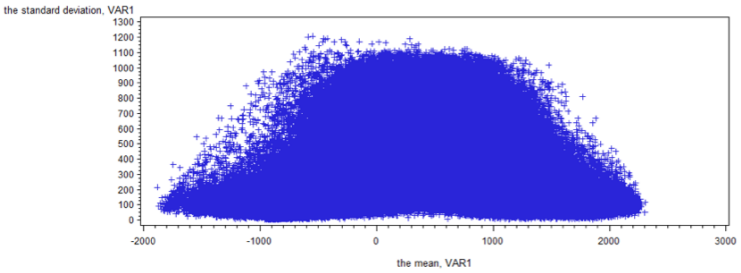

Figure 3: Scatterplot of mean and standard deviation of the intensity observed in a voxel. These statistics were taken voxel by voxel from 15 samples of a part provided to the working group; each point on the plot corresponds to a (mean, standard deviation) pair for one of these voxels.

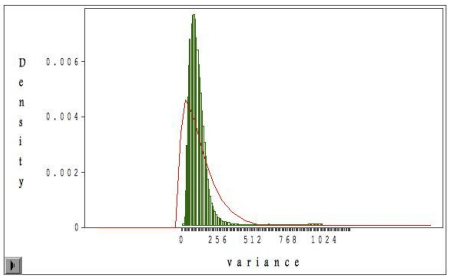

Figure 4: Histogram in the variance of the intensity in voxels, with statistics for each voxel computed from 15 samples of a part provided to the working group.

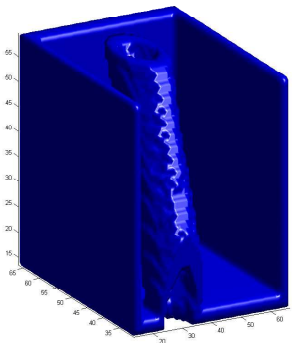

Figure 5: Toy model's surface

model, feeding it the actual model for the image and noise, as a first check of its potential. If the defect detection algorithm does not work well on the toy model, then one may move on to other ideas without taking time to see if the algorithm would work better under different models of the noise, etc. This therefore helps separates the research into two subtasks: developing an algorithm that works well when the statistics of the image and defects are known, then developing a model for the image and defects that works for the actual data under consideration.

We designed the toy model as a cube with a cylindrical hole entering and exiting the cube at opposite, nonadjacent faces of the cube (Figures 5 and 6). To incorporate acceptable manufacturing variations into the toy model, we allowed the radius, entry point, and exit point of the cylindrical hole to vary

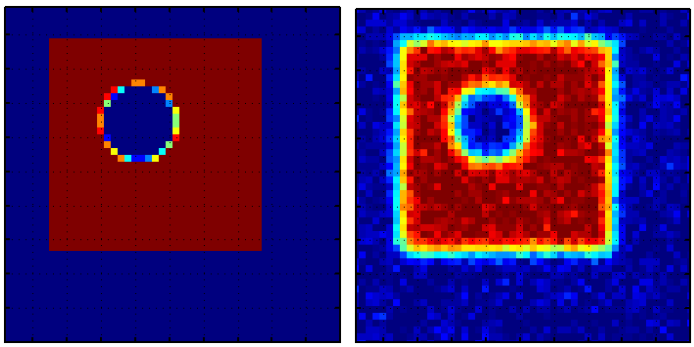

Figure 6: Cross section of voxel values in toy model before (left panel) and after (right panel) imaging artifacts are introduced

within manufacturing tolerances. These tolerances were assumed to be on the order of voxels, but we could exaggerate or depress them as desired.

To incorporate a particular manufacturing defect into our model, we introduced voids with locations generated by a Poisson point process and whose shape was generated by a short random walk. A more realistic variation of the model could employ a random choice from a library of defect shapes. The radius of the void was assumed to be about the order of a voxel, but we could again exaggerate or depress the size of the void as desired.

To incorporate the reduction of voxel intensity due to photon fatigue, which is known as shadowing, we adjusted the mean intensity $\bar{I}$ of a voxel $\vec{X}$ by

$$\bar{I}(\vec{X}) = e^{-\frac{d(\vec{X})}{l}},$$

where $d(\vec{X})$ was the shortest distance between voxel $\vec{X}$ and the edge of the cube and l was a parameter reflecting the rate of shadowing. We could vary the degree of shadowing in accordance with the properties of the part measured and the equipment measuring it, but we could not determine a suitable choice for l from the sample X-ray imagery.

To introduce noise from the imaging, we applied a normal model whose standard deviation was multiplicative with respect to intensity for regions of free space and solid material and additive with respect to intensity for intermediate regions. This was motivated by the sample X-ray imagery, where the standard deviation of the intensities appeared to be governed by

relationship

$$\sigma_I(\vec{X}) = \begin{cases} \frac{0.15}{0.25}\bar{I}(\vec{X}), & 0 \leq \bar{I}(\vec{X}) \leq 0.25 \\ 0.15, & 0.25 < \bar{I}(\vec{X}) < 0.75 \\ \frac{0.15}{0.25}\left(1 - \bar{I}(\vec{X})\right), & 0.75 \leq \bar{I}(\vec{X}) \leq 1 \end{cases} \tag{1}$$

where $\bar{I}(\vec{X})$ is the mean intensity of the voxel under consideration (see Section 2). To incorporate image reconstruction artifacts, we performed a weighted average of the intensity of each voxel with the intensities of adjacent and nearly adjacent voxels. We could not determine suitable weights for averaging from the sample X-ray imagery. Noise was added to each voxel according to the above prescription before and after introducing image reconstruction artifacts.

4 Geometric Approach

One natural way to check for defects is to develop a reference template for a given part, indicating where the material and void regions should be, and then checking the intensity profile of a given part against that template. What complicates this approach is that defect-free parts will themselves have acceptable variations, and simple changes in their orientation when imaged will cause significant differences in their voxel representation of intensity. Moreover, as discussed in Section 2, photon starvation effects and reconstruction artifacts imply that we cannot simply check whether material regions have intensities near 1 and void regions have intensities near 0. Finally, noise in the imaging and reconstruction will cause intensity fluctuations that we don't want to interpret as material defects.

Therefore, our geometric approach will adopt a statistical approach. Our general strategy will be to first construct a fattened reference surface which divides regions that should be material from regions that should be void, then to check for defects of various types according to the region of interest. We next provide some details on each of these two phases.

4.1 Construction of Reference Template Image

Figure 7 show the statistics of the intensity in a two-dimensional cross section taken from a collection of images of a part of a certain type. In the left

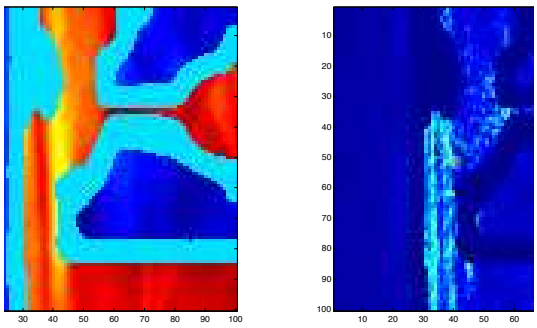

Figure 7: Mean (left panel) and standard deviation (right panel) of intensity of several images of a given part

panel, the higher intensity red regions correspond to material, while the lower intensity dark blue regions correspond to void. While any given part has a sharp surface dividing these two regions, the ensemble of images of parts of a given type have a rather broad light blue surface region. The reason for the fattening of this dividing surface in the statistical ensemble of images is variation between parts in different images, both due to actual variations in the structure (which are within acceptable tolerance) and differences in how the different parts are registered due to variations in their spatial orientations and positions when imaged. We see that if we were to take a sharp reference surface and demand that voxels inside that surface should have low intensity and voxels outside that surface should have high intensity, we would be prone to reject many parts as defective that are actually perfectly acceptable.

Therefore, we suggest constructing a reference template image as follows. First, we identify an ideal reference surface dividing the material from void regions in one of two ways. If we have a CAD model for the part's design, we can simply represent the ideal reference surface from those schematics. If we are not given an ideal design, then we can take the ensemble of images of various instances of the parts and compute the mean voxel intensity across those images (as in the left panel of Figure 7). We assume defects will be washed out in this statistical averaging, so that this averaged image is a reasonable representation of the intensity profile of an acceptable part. We then identify an idealized reference surface through some surface-detection algorithm, such as taking the surface as the collection of voxels with a given intermediate intensity value, or looking for regions with a large gradient in voxel intensity. In either case, the idealized reference surface is then dilated

into a fattened surface; the appropriate thickness can be inferred from the plot of mean intensity by identifying the width over which the voxel intensity remains away from 0 and 1, or from the plot of the standard deviation by taking the width of the region over which the standard deviation is substantial. All voxels within this fattened surface are then taken as surface voxels (S). We then label the remaining voxels as interior (I) or exterior (E) voxels through a flood fill procedure beginning with voxels on either side of this fattened reference surface.

4.2 Identification of Defects Given Reference Template

Once the reference template is obtained, we can look for defects of various types. We propose here two methods for identifying voids in material regions, but similar ideas could be developed to test for sand in regions that should be void, or cracks emanating from the surface. Our methods each take into account imaging artifacts and noise.

4.2.1 Test for Void Defect through Anomalously Low Intensities in Material Regions

A simple idea for looking for a void in a region that should be filled with material is to look for voxels with intensities that are too low. Were the voxel intensities to be ideal representations of the image, then we could simply test whether interior voxels have intensities close enough to 1. But for reasons discussed previously in Section 2, such an approach would clearly produce too many false positives because the intensity of an interior voxel could be well below 1, without representing a defect, due to being in a photon-starved region deep in the interior or due to noise fluctuations. To build a test with more specificity, we supplement our geometric decomposition of the image with:

- a reference intensity profile $\bar{I}(\vec{X})$, representing the expected intensity of each voxel $\vec{X}$
- the standard deviation $\sigma_I(\vec{X})$ of the intensity of each voxel $\vec{X}$ due to imaging and reconstruction

We could obtain these functions in either an analytical or statistical way. The analytical approach would be to devise an algorithm that would calculate,

given the geometry of the material region, what intensity each voxel should have based on photon starvation effects, and use this for $\bar{I}(\vec{X})$. The standard deviation function $\sigma_I(\vec{X})$ could be then inferred from a noise model such as in Eq. (2). Alternatively, if we are given a collection of images of parts of a given type, we can simply take these as a statistical ensemble and compute the mean and standard deviation of each voxel, excluding outliers, as we did in Section 2.

Once we have the functions $\bar{I}(\vec{X})$ and $\sigma_I(\vec{X})$, we would flag a possible defect at voxel $\vec{X}$ if its intensity $I(\vec{X})$ in a given image satisfied:

$$I(\vec{X}) < \bar{I}(\vec{X}) - c\sigma_I(\vec{X}),$$

where c is some constant that would be chosen, probably through trial and error. The idea is that we are suspicious of a voxel if its intensity is too many standard deviations below the expected intensity. When we applied this algorithm to a test problem, it flagged quite a few spurious defects, but many of these could be discarded from consideration if we were to ignore suspicious voxels that are isolated (have no neighbors that are also suspicious). The motivation for such an approach is that a void should have some finite volume and be likely to contaminate some contiguous set of voxels, so an isolated voxel with anomalously low intensity is likely to be due to an imaging artifact rather than a true defect in the material.

4.2.2 Test for Void Defect by Hypothesis Comparison

An alternative approach for testing for void defects in a material region is to consider whether the intensity of a voxel in a given image is more compatible with the hypothesis of material in that region or void in that region. This would require us to obtain first a reference intensity function $\bar{I}(\vec{X})$ as in the previous method, which would describe the intensity value we would expect if the voxel actually corresponding to material, as it should. We would also need a function $I^V(\vec{X})$ that would describe the intensity value we would expect at voxel $\vec{X}$ if it corresponded to a void. Whereas $\bar{I}(\vec{X})$ could be obtained by either an analytical or statistical approach, as described in the previous method, the function $I^V(\vec{X})$ must be obtained from some analytical basis since we cannot expect to have a collection of parts all of which have a void at a given location. One way that the function $I^V(\vec{X})$ might be constructed is to take a weighted average of 0 and the reference intensity $\bar{I}(\vec{X})$, to model

reconstruction artifacts that would give some intensity to a voxel in a void due to smoothing from nearby regions. More sophisticated models for $I^V(\vec{X})$ might be developed from better understanding of the imaging process.

Once the functions $\bar{I}(\vec{X})$ and $I^V(\vec{X})$ are obtained, we would flag a void defect at an intenior voxel when its intensity at a given part satisfies:

$$I(\vec{X}) < \frac{I^V(\vec{X}) + \bar{I}(\vec{X})}{2},$$

that is the intensity is closer to what would be expected under the hypothesis of a void than under the hypothesis that the voxel corresponds to a material region. We are assuming here that the noise levels under these two competing hypotheses are comparable, so that the midpoint of their expected intensities provides a reasonable discrimination point. To do better, we would have to develop a noise model under the hypothesis of a void at voxel $\vec{X}$, for which we had no particularly promising ideas. As with the previous method, we would suggest discarding from consideration isolatd flagged voxels.

5 Basis Expansion Approach

An approach different from the geometric one above is to expand the volumetric data in terms of one or more bases, such as wavelets, Fourier modes, or curvelets. Representing the data in a different domain may facilitate the detection of defects, since defects might be more easily distinguished from normal features in a suitable representation. We will focus our discussion on curvelets, since they seem to be the most promising avenue.

5.1 Curvelets

Just a decade old, curvelets are a basis of functions well adapted for representing images defined by smooth curves, perhaps with some singularities like intersections [2]. The edges produced by simple images can create some challenges for Fourier and even more classical wavelet bases, since a simple edge may project substantially onto a large set of modes. The problem is the anisotropy implicit in edges – very thin in one direction with more gradual variation in the other(s), and this anisotropy need not line up with the axes on which the Fourier or wavelet modes are based. Curvelets were designed to be much better adapted in parsimoniously representing images with simple

curves in arbitrary directions, so in particular objects such as cartoons and text can be well represented using few curvelets. We remark that though its name suggests a two-dimensional representation, the use of curvelets have been extended to higher dimensions (in particular to dealing with curves and surfaces in three dimensions) [19]. What characterizes 3D curvelets is that they are short in at least one dimension and potentially long in the others (Figure 8). That is, they can be long, skinny tubes, curved surfaces, or tightly coiled balls.

Most normal features of the manufactured parts should be surfaces, and so images of normal parts should, in the curvelet domain, concentrate their amplitudes on curvelets that represent surfaces. By contrast, voids would be best represented by curvelets that are small in all three dimensions, i.e., small balls or ellipsoids (or other localized shapes). As a result, whenever the curvelet expansion has a particularly large amplitude of coefficients corresponding to curvelets that are small in all dimensions, these images could be flagged as suspected defects. Inverting the curvelet transform from the projection onto these modes could help identify the location of the defect, though this may not be necessary if the purpose of image processing is to simply flag a suspicious image rather than point to the particular area of suspicion. Determining the appropriate threshold amplitudes for flagging a defect would require experimentation.

While this procedure may work well for void and wormwhole defects, which are localized in all three dimensions, other defects such as cracks may be more difficult to distinguish in the curvelet domain because they are spatially extended in one dimension but not in the other two. Curvelets should be able to distinguish such features from normal smooth surfaces, but confusion could arise with thin "necks" in the metal of a part, which is likely to project onto simliar curvelet modes. The discrimination here may require a determination of the normal mode amplitudes and phases for the curvelets representing images of acceptable parts, and then checking when the projection of an image onto these modes deviates more than an acceptable threshold (due to part-to-part variation) from the "normal values." Of course trying to detect deviations of mode amplitudes and phases from certain "normal values" will be more challenging than simply checking whether certain mode amplitudes exceed a certain low threshold, so crack detection by curvelets could be expected to be subtle.

Expanding data in the 3D curvelet domain appears to be computationally feasible given the time constraints, as shown in Table 1.

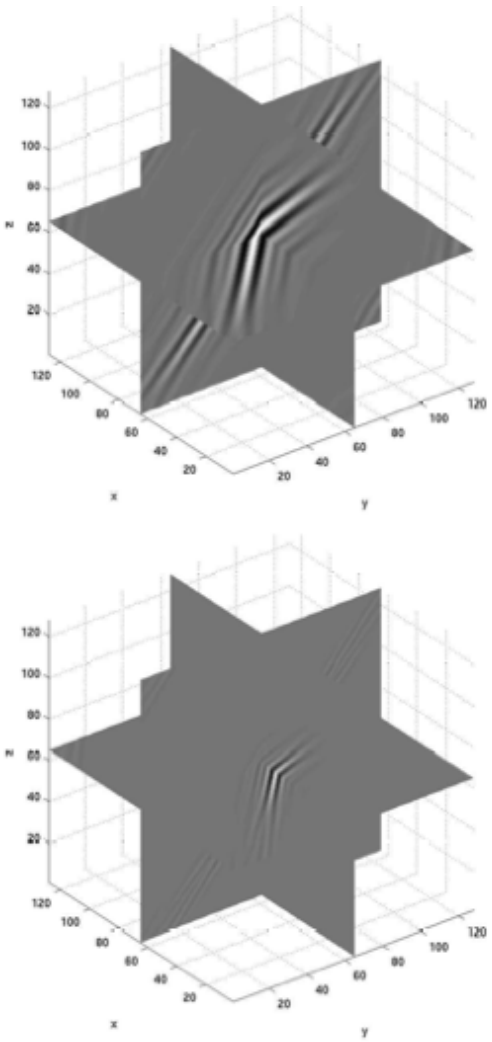

Figure 8: Two 3D curvelets, one large in scale and one small [19].

Table 1: Computation speed of 3D curvelet transform on a supercomputer in 2005 (from Ying et al. [19]).

Grid size	Number of Processors	Time
256^3	4	47 sec
512^3	32	50 sec
1024^3	128	94 sec

5.2 Frames and Sparse Representations

Another potentially fruitful approach is to use *frames*, or sets of vectors that span the space but may be linearly independent or dependent. A frame could consist of two orthogonal bases, such as wavelets and curvelets; their union is an over-abundance of basis vectors, and therefore no longer a basis. However, combining two bases could be useful because images may be well represented by a combination of a few basis elements from different bases. (Think of an image of a face: curvelets better represent some features, such as contours of the face, whereas more classical wavelets better represent other features, such as glasses or pupils..)

Consider a frame consisting of 3D wavelets and 3D curvelets, for example. To expand the volumetric data in terms of this frame is highly underdetermined: there are many different ways to represent the data in terms of these curvelets and wavelets. However, it may be possible to represent the data in terms of very few curvelets and wavelets—a so-called "sparse representation".

The past decade has seen a flourishing of advances in techniques for finding sparse solutions (and in understanding the probability of finding them, which requires sophisticated mathematics). Techniques in convex programming, such as *basis pursuit*, can search for sparse representations in a frame; one useful implementation can be found in Grant and Boyd [4]. For a popular science introduction to compressive sensing, see Ellenberg [3]. An extensive list of resources on compressive sensing is maintained by a research group at Rice University [5], while a thorough introduction to compressive sensing can be found in [1].

Suppose there is a basis well suited for the features of an object but not for the defects (perhaps 3D curvelets), while another basis is well suited for the defects but not the features (perhaps 3D wavelets). Determining whether two

such bases exist in a practical sense would require experimentation. Supposing they have been established, then techniques in compressive sensing could seek a sparse representation of the data (by minimizing the ℓ_2-norm, for example). Then in the sparse representation, the hope is that the defects would concentrate their amplitudes in one basis, while features would concentrate their amplitudes in the other basis—hence facilitating detection of defects. Whether finding the sparse representation of the frame is computationally feasible in the minute-scale time constraint is unclear, though it appears to be in the realm of feasibility. Ideas along these lines have been applied recently to defect detection in textures [8, 9, 13, 16], fabrics [6, 10, 11, 14, 15, 18] and chips [7, 17].

6 Topological Approach

A qualitatively different approach, which we did not pursue in the workshop, is to attempt to explore whether the image is topologically consistent with the ideal part. This approach would be best suited for detecting material defects (sand) in regions that should be void. From a reference template, one would sketch out a branching path of line segments that would "explore" the void regions in the part. On a given image, one would attempt to draw a similar branching path that would only encounter voxels with sufficiently low intensity (which would be assumed to correspond to a void region.) Because of part-to-part variation and registration issues, we wouldn't insist that the branching path also fits in each image perfectly; we would only ask that it fit topologically. That is, we don't prescribe the lengths of the branching segments, but just whether it is possible to construct a tree with the same kind of branchings, with each branch having some minimal length. A channel obstructed by sand would presumably fail such a test. This does leave open the question of how to check that a given voxel representation, especially in three dimensions, is consistent with a certain branching topology of void space. Perhaps one could start with the reference branching path, including lengths, and if that path hit high intensity voxels (that are probably not an actual void region), then iteratively adjust the branching segment lengths to see if the reference branching tree can be shuffled into purely low-intensity voxels without changing or losing any of the fundamental turns or branches.

7 Conclusions and Directions for Future Work

The workshop has provided hopefully some new perspectives on methods for automatically detecting defects in parts from scanned three-dimensional images. Part-to-part variations and noise in the imaging and reconstruction process seem to suggest that a statistically-based approach is necessary. To this end, we have conducted some preliminary statistical analysis of some sample images provided to us to get a sense of the noisiness of the intensities in a set of images of various instances of a given part. We also developed a mathematical toy model that could be used for testing and exploring algorithmic approaches in a highly controlled context, before subjecting them to the large number of unknown variables characteristic of real data. We have suggested three methodologies that seem viable for further exploration: 1) a geometric approach which decomposes the image into surface, interior, and exterior regions, and checks that each voxel behaves as it should within its region, 2) a basis expansion approach in which we check whether the image has a nontrivial projection onto modes that are associated to defects, and 3) a topological approach for detecting sand occlusions of regions that should be void by attempting to fit a branching path through purely low-intensity voxels. The week of the workshop did not permit us to test any of these ideas in great depth, but we would suggest beginning with tests on very simple examples, such as our mathematical toy model, to see the fundamental strengths and weaknesses of an approach before confounding the challenge with the extra unpredicatibility of real data. Of course any workable algorithm must work well with real data, but the use of the mathematical model as an intermediate step may suggest ways to refine or adjust an approach that might otherwise be discarded when it is simply tried on data and found not to work as designed.

We close by mentioning a couple of ideas that emerged at the workshop but were not developed with any details:

- The defect detection algorithms suggested here probably are excessively aggressive, and can be expected only to suggest suspicious voxels. Likely, some of these suspicious candidates should be automatically pruned from consideration if, for example, an insufficient number of the neighboring voxels are also flagged as suspicious.

- The defects are modeled in Section 3 as localized void regions. A model for crack defects could be constructed by selecting a random material

location as a crack initiation site, from which the crack propagates according to a random walk until it terminates when it reaches a voxel corresponding to a material edge.

References

[1] Compressive sensing: The big picture. URL `http://sites.google.com/site/igorcarron2/cs`.

[2] E. Candes, L. Demanet, D. Donoho, and L. Ying. Fast discrete curvelet transforms. *SIAM Multiscale Model. Simul.*, 5(3):861–899, 2006.

[3] Jordan Ellenberg. Fill in the blanks: Using math to turn lo-res datasets into hi-res samples. URL `http://www.wired.com/magazine/2010/02/ff_algorithm/all/1`.

[4] Michael Grant and Stephen Boyd. Cvx: Matlab software for disciplined convex programming. URL `http://cvxr.com/cvx/`.

[5] Rice University Compressed Sensing group. Compressed sensing resources. URL `http://dsp.rice.edu/cs`.

[6] Shengqi Guan, Xiuhua Shi, Haiying Cui, and Yuqin Song. Fabric defect detection based on wavelet characteristics. In *Computational Intelligence and Industrial Application, 2008. PACIIA '08. Pacific-Asia Workshop on*, volume 1, pages 366–370, 2008.

[7] Fanzhi Kong and Hongsheng Ni. Defect recognition algorithm based on curvelet moment and support vector machine. In *E-Health Networking, Digital Ecosystems and Technologies (EDT), 2010 International Conference on*, volume 1, pages 142–145, 2010.

[8] A. Kumar and G.K.H. Pang. Defect detection in textured materials using gabor filters. *Industry Applications, IEEE Transactions on*, 38(2): 425–440, 2002. ISSN 0093-9994.

[9] G. Lambert and F. Bock. Wavelet methods for texture defect detection. In *Image Processing, 1997. Proceedings., International Conference on*, volume 3, pages 201–204 vol.3, 1997.

[10] Jianli Liu and Baoqi Zuo. The recognition of fabric defects using wavelet texture analysis and LVQ neural network. In *Image and Signal Processing, 2009. CISP '09. 2nd International Congress on*, pages 1–5, 2009.

[11] Jing Luo, Jian-yun Ni, Shu-zhong Lin, and Li-mei Song. A noise filtration technique for fabric defects image using curvelet transform domain filters. In Zhengyu Du and Bin Liu, editors, *Proc. of SPIE*, volume 7820, pages 78202E–78202E–6, Xi'an, China, 2010. doi: 10.1117/12.866962. URL `http://link.aip.org/link/PSISDG/v7820/i1/p78202E/s1&Agg=doi`.

[12] D. Mery, T. Jaeger, and D. Filbert. A review of methods for automated recognition of casting defects. *INSIGHT-WIGSTON THEN NORTHAMPTON-*, 44(7):428–436, 2002.

[13] B. B. M. Moasheri and S. Azadinia. A new voting approach to texture defect detection based on multiresolutional decomposition. *World Academy of Science, Engineering, and Technology*, 73:657–661, jan 2011.

[14] Henry Y.T. Ngan, Grantham K.H. Pang, S.P. Yung, and Michael K. Ng. Wavelet based methods on patterned fabric defect detection. *Pattern Recognition*, 38(4):559–576, April 2005. ISSN 0031-3203. doi: doi:10.1016/j.patcog.2004.07.009. URL `http://www.sciencedirect.com/science/article/pii/S0031320304003693`.

[15] Henry Y.T. Ngan, Grantham K.H. Pang, and Nelson H.C. Yung. Automated fabric defect detection–A review. *Image and Vision Computing*, 29(7):442–458, June 2011. ISSN 0262-8856. doi: doi:10.1016/j.imavis.2011.02.002. URL `http://www.sciencedirect.com/science/article/pii/S0262885611000230`.

[16] Du-Ming Tsai and Cheng-Huei Chiang. Automatic band selection for wavelet reconstruction in the application of defect detection. *Image and Vision Computing*, 21(5):413–431, May 2003. ISSN 0262-8856. doi: doi:10.1016/S0262-8856(03)00003-9. URL `http://www.sciencedirect.com/science/article/pii/S0262885603000039`.

[17] Qingxiang Wang, Di Li, Wujie Zhang, Dong Cao, and Hao Chen. Unsupervised defect detection of flexible printed circuit board gold surfaces based on wavelet packet frame. In *Industrial and Information Systems*

(IIS), 2010 2nd International Conference on, volume 2, pages 324–327, 2010.

[18] Yean Yin, Wen Bing Lu, Ke Zhang, and Liang Jing. Textile flaw detection and classification by wavelet reconstruction and BP neural network. In *Intelligent Systems, 2009. GCIS '09. WRI Global Congress on*, volume 4, pages 167–171, 2009.

[19] L. Ying, L. Demanet, and E. Candes. 3d discrete curvelet transform. In *Proc. SPIE wavelets XI, San Diego*, page 591413. Citeseer, 2005.